An Equivalent Circuit Model for Terminated Hybrid-Mode Multiconductor Transmission Lines

LAWRENCE CARIN AND KEVIN J. WEBB, MEMBER, IEEE

Abstract—**An equivalent circuit for terminated hybrid-mode multiconductor transmission lines is presented. Existing CAD packages, such as SPICE, can be used for its implementation. Model parameters can be found from either a TEM or a full-wave analysis of the transmission lines. The equivalent circuit is used to simulate multiconductor microstrip for applications in high-speed integrated circuits. An examination of the validity of the TEM approximation for example cases is carried out in the time and frequency domains.**

I. INTRODUCTION

MICROSTRIP transmission lines have been the subject of extensive study for many years. However, the various terms used to describe the microstrip modes are often not clearly delineated. For clarity, it is necessary that the different identifications for the microstrip modes be explicitly defined. In this paper a TEM mode is defined as one with zero or negligible longitudinal fields and no dispersion; a quasi-TEM mode has negligible longitudinal fields but is not dispersionless; and a hybrid mode has both dispersion and all six field components. The TEM and quasi-TEM modes are special cases of the hybrid mode, and the classification of a given mode as TEM or quasi-TEM often will depend on the frequency range of interest. Microstrip embedded in an inhomogeneous medium supports only hybrid modes. However, at sufficiently low frequencies the propagating hybrid modes have small longitudinal field components relative to the transverse fields. For this reason microstrip lines are often analyzed under the assumption that the longitudinal fields can be neglected. This has contributed to the structure's popularity, as by neglecting the longitudinal fields one can define line voltage and current compatible with ordinary lumped circuit devices. Since the longitudinal fields are neglected, the transmission line parameters are usually found in terms of per-unit-length inductance and capacitance matrices calculated through a dc electric and magnetic analysis [1]. Such an analysis will be referred to in this paper as a TEM calculation of the microstrip parameters (mode velocities, eigencurrents, and eigenvoltages). This is a frequency-independent analysis and therefore one obtains TEM modes. The longitudinal variation of voltage and current on the TEM microstrip is described by telegraphist's equations [2]. Frequency-dependent voltage and current using a quasi-TEM approach can be simulated approximately by assuming frequency-dependent inductance and capacitance matrices [3]. However, as digital integrated circuits get faster, the pulse rise and fall times will become shorter and thus their frequency spectrum will extend into the millimeter-wave regime. The assumption that the longitudinal fields are negligible is less accurate as frequency increases. For these high-frequency cases a full-wave analysis is required to validate that the longitudinal fields can be neglected, and when deemed appropriate it can be used to define quasi-TEM parameters that accurately depict the frequency dependence of the lines.

A full-wave method, such as the spectral-domain technique [4], accurately models frequency-dependent microstrip. Using the spectral-domain technique one assumes the lines are infinitesimally thin and that the conductors are lossless. After solving for the true hybrid modes, one can determine if the longitudinal fields are negligible relative to the transverse fields, and if appropriate a quasi-TEM analysis can be employed to describe the longitudinal variation (propagation) of the modes. The approximate quasi-TEM analysis is desired as opposed to continuing with the rigorous full-wave approach (after finding the hybrid modes) because the line terminations are usually described by circuit quantities (voltage and current) rather than by the more general field quantities [5]. Thus the full-wave technique is used to find the frequency-dependent microstrip parameters (line currents, modal power, and complex modal propagation constants), and when appropriate these are then used to define equivalent quasi-TEM voltages and currents. Since the voltage cannot be defined uniquely in terms of an integral of electric field, it is defined indirectly through a characteristic impedance which relates voltage to current. This characteristic impedance itself cannot be uniquely defined since the modes are hybrid, but well-accepted definitions are avail-

Manuscript received July 11, 1988; revised June 28, 1989. This work was supported in part by grants from the Semiconductor Research Corporation and Martin Marietta Laboratories.

L. Carin was with the Electrical Engineering Department, University of Maryland, College Park. He is now with the Polytechnic Institute of New York, 333 Jay St., Brooklyn, NY 11201.

K. J. Webb is with the Electrical Engineering Department, University of Maryland, College Park, MD 20742.

IEEE Log Number 8930653.

0018-9480/89/1100-1784$01.00 ©1989 IEEE

able in the literature [6]–[8]. In this way one obtains frequency-dependent microstrip parameters (found from a rigorous full-wave solution) which are compatible with standard lumped circuit models. The benefit inherent in using a full-wave technique is that one evaluates the true hybrid microstrip fields and then determines the accuracy of using a TEM or a quasi-TEM analysis. As the frequency of operation gets higher, the modes start to deviate too far from quasi-TEM modes (negligible longitudinal fields) and one must analyze the problem from the field rather than the circuit point of view [9].

Since multiconductor microstrip is a common component in integrated circuits, there has been much work done to simulate signal propagation on such lines. Almost all have relied on the telegraphist's equations which use inductance and capacitance matrices. Using these equations, Chang [2] has shown that one can decouple a system of N coupled microstrip lines into a set of N decoupled TEM modes. The system of coupled lines can then be analyzed by using congruence transformers to couple these modes at terminations. Tripathi [10] has used this approach to incorporate the analysis of lossless, dispersionless multiconductor transmission lines with SPICE by using dependent voltage and current sources at terminations instead of transformers. These approaches, as well as many others [11], [12], rely on the telegraphist's equations and the corresponding inductance and capacitance matrices.

Djordjevic *et al.* [3] used a time-dependent Green's function and augmented lines terminations to model frequency-dependent, lossy multiconductor transmission lines. Although in [3] the Green's function was determined through inductance and capacitance matrices, it could also be determined from frequency-dependent parameters found through a full-wave analysis. This approach, although rigorous and general, can be complicated to use due to the need to find appropriate matching networks for the terminations. Additionally, the model is not readily compatible with existing CAD package such as SPICE since it requires the computation and storage of a time-dependent Green's function. Tripathi [13] has presented a model compatible with SPICE to simulate time-harmonic signal propagation on lossy, dispersive multiconductor transmission lines. This model, however, requires the decoupled modes to be characterized by a cascade of lumped elements between ideal (lossless and dispersionless) transmission lines. In [13] each decoupled line is represented by 16 cascaded lumped element sections. This results in an equivalent circuit that must be modified with changing line lengths and operating frequencies. In this paper a new model for multiconductor microstrip is presented. The model is similar to that in [10] but is compatible with a full-wave or TEM solution for the multiconductor microstrip parameters. Unlike the model in [13], the form of the equivalent circuit is independent of line length and frequency of operation. It is implemented here by using SPICE and therefore can analyze lossless, dispersive linearly loaded lines and lossless, nondispersive nonlinearly loaded lines. The capabilities of the model are limited in this implementation by the fact that SPICE currently analyzes only dispersionless and lossless single transmission lines. If another CAD package more powerful than SPICE were used (capable of analyzing lossy single transmission lines), loss could also be included in the equivalent circuit model.

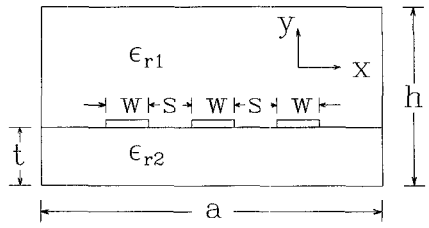

Fig. 1. Three shielded microstrip lines on a single substrate. Geometry studied has parameters $w = 1.524$ mm, $s = 0.254$ mm, $t = 0.254$ mm, $h = 2.54$ cm, and $a = 2.54$ cm, $\epsilon_{r1} = 1$, $\epsilon_{r2} = 4.65$.

The paper begins by deriving an equivalent circuit model for multiconductor microstrip. It is shown that the model can be easily incorporated into existing software packages such as SPICE. An explanation is given as to how the model is compatible with either a TEM or a full-wave-based solution of the microstrip parameters. An example case previously examined in the literature is analyzed to validate the model's accuracy. Several examples are considered for a dispersive, asymmetric, dual-level coupled microstrip geometry. Results are given for time-harmonic as well as pulse signal propagation on the coupled microstrip.

II. Circuit Model

Consider a multiconductor shielded microstrip geometry such as that in Fig. 1. For a geometry with N strips (plus ground) there are N fundamental zero-cutoff-frequency modes. These are commonly referred to as TEM or quasi-TEM modes because at low enough frequencies the longitudinal components of electric and magnetic field are negligible compared to the corresponding transverse fields. For simplicity, throughout the derivation of the model the fields are assumed to be time-harmonic and the time dependence $e^{j\omega t}$ is suppressed. However, after the model is derived it will be shown that the equivalent circuit is capable of describing the propagation of more general signals. Let the current on line k for mode j be denoted i_{kj}, where $j = 1,2,\ldots, N$ and $k = 1,2,\ldots, N$. Using bra-ket notation, an eigencurrent $|i_j\rangle$ is defined for mode j as

$$|i_j\rangle = \sum_{k=1}^{N} i_{kj}|k\rangle \tag{1}$$

where $|k\rangle$ corresponds to line k. A corresponding eigenvoltage $|v_j\rangle$ can be defined as

$$|v_j\rangle = \sum_{k=1}^{N} v_{kj}|k\rangle \tag{2}$$

where v_{kj} is the voltage of line k for mode j with respect to a reference conductor. The eigencurrents and eigenvoltages can be related via modal characteristic impedances Z_{kj}, where $v_{kj} = Z_{kj} i_{kj}$. The eigencurrents, eigenvoltages,

modal characteristic impedances, and propagation constants can be determined under the TEM assumption using inductance and capacitance matrices [1], [2] or from a general full-wave technique [4], [5], as will be shown in the next section.

The eigenkets $|i_j\rangle$ and $|v_j\rangle$ are unique to within a common multiplicative constant determined by the boundary and initial conditions. The total voltage and current on the lines are superpositions of the different eigenkets:

$$|i_T\rangle = \sum_{j=1}^{N} a_j|i_j\rangle = \sum_{j=1}^{N} a_j \sum_{k=1}^{N} i_{kj}|k\rangle \tag{3}$$

$$|v_T\rangle = \sum_{j=1}^{N} a_j|v_j\rangle = \sum_{j=1}^{N} a_j \sum_{k=1}^{N} i_{kj}Z_{kj}|k\rangle \tag{4}$$

where a_j is the mode coefficient for mode j, as determined by the boundary and initial conditions. The kets $|i_T\rangle$ and $|v_T\rangle$ represent the total currents and voltages, respectively, on the lines at point z. Since there is one mode coefficient for each mode in (3) and (4), these equations pertain to signals traveling in one direction with no reflection. When reflection is subsequently considered for terminated microstrip, each mode j will have forward ($a_j^{(+)}$) and backward ($a_j^{(-)}$) mode coefficients with corresponding propagation constants ($e^{\mp j\beta_j z}$) to represent the forward and backward propagation of a given mode. The total current and voltage on line k at point z are, respectively,

$$\langle k|i_T\rangle = \sum_{j=1}^{N} a_j i_{kj} \tag{5a}$$

and

$$\langle k|v_T\rangle = \sum_{j=1}^{N} a_j i_{kj} Z_{kj}. \tag{5b}$$

The total voltages and currents can be written in matrix form as

$$\begin{aligned} \boldsymbol{I}\boldsymbol{a} &= \boldsymbol{i}_T \\ \boldsymbol{V}\boldsymbol{a} &= \boldsymbol{v}_T \end{aligned} \tag{6}$$

where $\boldsymbol{I}$ and $\boldsymbol{V}$ are $N \times N$ matrices with components i_{kj} and $i_{kj}Z_{kj}$ (row k, column j), respectively. The N-dimensional column vectors $\boldsymbol{i}_T$ and $\boldsymbol{v}_T$ are the total voltages and currents on the N lines as defined in (5a) and (5b), respectively, and $\boldsymbol{a}$ is a column vector representing the mode coefficients. The total voltage and current, $\boldsymbol{v}_T$ and $\boldsymbol{i}_T$, depend solely on $a_1, a_2, \cdots, a_N$, which change with spatial position according to the phase factor of the given mode, i.e.,

$$a_j(z+l) = a_j(z)e^{-j\beta_j l} \tag{7}$$

for mode j propagating a distance l in the positive z direction.

Considering terminated microstrip, it is possible to model the system of transmission lines with equivalent decoupled lines of unit characteristic impedance. This is seen by defining the equivalent voltage for mode j as

$$v_j = a_j^{(+)}e^{-j\beta_j z} + a_j^{(-)}e^{j\beta_j z} \tag{8}$$

and the current as

$$i_j = a_j^{(+)}e^{-j\beta_j z} - a_j^{(-)}e^{j\beta_j z} \tag{9}$$

with β_j being the propagation constant for mode j. These equations describe the spatial variation of the mode coefficients for mode j. Each mode j is modeled with equivalent decoupled transmission lines of unit characteristic impedance and propagation constant (time delay) coming from the full-wave or TEM analysis of mode j.

The total true voltages and currents of the terminated lines are related to these equivalent voltages and currents through (6). It is therefore seen that

$$\begin{aligned} \boldsymbol{I}\boldsymbol{i} &= \boldsymbol{i}_T \\ \boldsymbol{V}\boldsymbol{v} &= \boldsymbol{v}_T \end{aligned} \tag{10}$$

where $\boldsymbol{i}$ and $\boldsymbol{v}$ are N-dimensional column vectors that represent the modal coefficients with components given by (8) and (9) and correspond to the transmission line modal quantities. Now, $\boldsymbol{i}_T$ and $\boldsymbol{v}_T$ represent the total current and voltage, respectively, at point z for terminated microstrip with forward and backward traveling modes. The equivalent decoupled transmission lines described by $\boldsymbol{i}$ and $\boldsymbol{v}$ are related to the voltages and currents at all points on the physical lines by $\boldsymbol{I}$ and $\boldsymbol{V}$. Since (10) is valid at all points z, the circuit model for the multiple lines will be formulated by imposing these coupling conditions at the terminations, $z = 0$ and $z = l$, where l is the line length. Thus $\boldsymbol{I}$ and $\boldsymbol{V}$ are used at the terminations as couplers of the N decoupled equivalent transmission lines of unit characteristic impedance to represent the N physical coupled lines. To construct the equivalent circuit model, consider

$$\begin{aligned} \boldsymbol{i} &= \boldsymbol{I}^{-1}\boldsymbol{i}_T \\ \boldsymbol{v}_T &= \boldsymbol{V}\boldsymbol{v}. \end{aligned} \tag{11}$$

If the matrix components of $\boldsymbol{I}^{-1}$ and $\boldsymbol{V}$ are labeled by b_{ik} and v_{ik} (row i, column k), respectively, the desired equivalent circuit can be represented as shown in Fig. 2.

The generality of the model is dictated by the capabilities of the CAD package with which it is implemented. Currently, SPICE can handle lossless, dispersionless single transmission lines. Using SPICE the model can handle arbitrarily loaded (linear or nonlinear) lossless, dispersionless multiconductor microstrip. If one considers only linear loads, the model can be extended to handle dispersion. This is done by using SPICE to sweep the frequency range of interest as the frequency-dependent model parameters are varied accordingly. An inverse FFT is then used to take the frequency-domain data from SPICE into the time domain to study dispersive signal propagation on linearly loaded multiconductor microstrip. Touchstone [14] uses a frequency-dependent attenuation constant to analyze lossy single lines. Thus if the model were implemented using Touchstone rather than SPICE, loss could also be included by using an attenuation constant in each decoupled transmission line corresponding to the attenuation of the mode each line simulates.

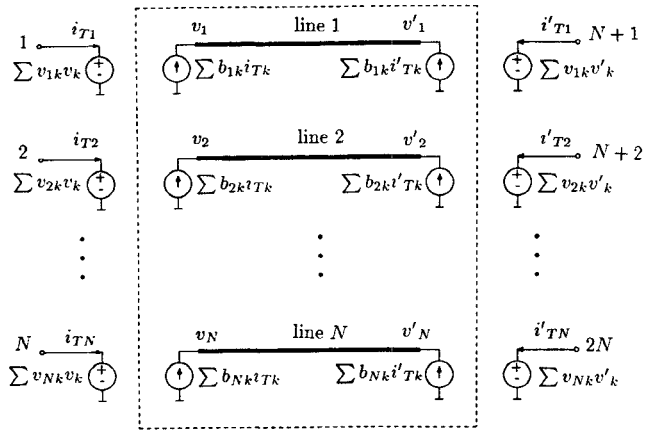

Fig. 2. Circuit model for N coupled microstrip lines. The N equivalent decoupled lines in the box represent the propagation of the N modes and they are coupled at the terminations by the dependent sources. The physical ports of the true lines are labeled 1 to N and $N+1$ to $2N$ on the two ends of the lines. All summations are for $k=1$ to N.

The main advantage of this model over those presented previously [2], [10]–[12] is that it is not restricted to the analysis of multiconductor microstrip using parameters from a TEM analysis of the transmission lines. The form of the model remains the same regardless of whether the model parameters are determined from a full-wave or a TEM solution. Thus results from the full-wave approach can easily be used to check those using the TEM approximation. Unlike the frequency-dependent model in [13], no complicated equivalent circuits of cascaded lumped elements are required to simulate the decoupled lines. Additionally, the model in [13] requires an extra step, not required in the present model, to synthesize the equivalent lumped elements after the frequency-dependent eigencurrents, eigenvoltages, and propagation constants have been determined.

III. Model Parameters

The circuit model presented in the previous section is compatible with a TEM or a full-wave solution for the multiconductor parameters. Since the TEM [1], [2] and full-wave analysis [4], [5] of microstrip have been studied extensively in the literature, only the essential details of each will be presented here. The presentation will be restricted to the lossless case, although, as mentioned above, loss could also be included.

A. TEM

Under the TEM assumption, the voltage and current on the N lines are described by the transmission line equations

$$\frac{\partial}{\partial z}\boldsymbol{v} = -\boldsymbol{L}\frac{\partial}{\partial t}\boldsymbol{i} \tag{12a}$$

$$\frac{\partial}{\partial z}\boldsymbol{i} = -\boldsymbol{C}\frac{\partial}{\partial t}\boldsymbol{v} \tag{12b}$$

where $\boldsymbol{i}$ and $\boldsymbol{v}$ are N-dimensional eigenvectors representing the currents and voltages, respectively, on the N lines, and $\boldsymbol{L}$ and $\boldsymbol{C}$ are per-unit-length $N \times N$ inductance and capacitance matrices, respectively. The capacitance matrix is found using static electric field analysis, and the inductance matrix is determined from the capacitance matrix for the geometry with all dielectrics replaced with free space [1]. Assuming an $e^{j(\omega t-\beta z)}$ t and z variation for $\boldsymbol{i}$ and $\boldsymbol{v}$, (12a) and (12b) can be rearranged to yield

$$(\boldsymbol{LC}-\lambda\boldsymbol{U})\boldsymbol{v}=0 \tag{13a}$$

$$(\boldsymbol{CL}-\lambda\boldsymbol{U})\boldsymbol{i}=0 \tag{13b}$$

where $\lambda=(\beta/\omega)^2$ and $\boldsymbol{U}$ is the unit matrix. The eigencurrents and eigenvoltages share the same eigenvalues [15]. Thus, one can solve (13a) and (13b) for the N eigenvoltages and eigencurrents with corresponding propagation constant $\beta=\omega\sqrt{\lambda}$. The eigenvoltages, eigencurrents, and propagation constants are used to construct the equivalent circuit.

B. Full-Wave

The spectral-domain technique with a method of moments solution is used for the full-wave analysis of multiconductor microstrip [4]. By working in the spectral domain, one obtains an equation of the form

$$\boldsymbol{Zc}=0 \tag{14}$$

where for a geometry of N lines $\boldsymbol{Z}$ is an $N(m_x+m_z)\times N(m_x+m_z)$ matrix, where m_x and m_z are the number of basis functions used to represent the x- and z-directed surface current densities, respectively, and $\boldsymbol{c}$ is an $N(m_x+m_z)$-dimensional vector representing the basis function coefficients for the surface current density. By setting the determinant of $\boldsymbol{Z}$ equal to zero one can determine the propagation constants for the N fundamental modes of the microstrip (as well as all evanescent modes). These eigenvalues are then substituted back into $\boldsymbol{Z}$ to solve for the relative basis function coefficients, $\boldsymbol{c}$. Once the current density is known, one can solve for the six field components associated with each mode. The current on line k for mode j is defined as

$$i_{kj}=\int_{S_k}\sum_{l=1}^{m_z} c_{lk}^{(j)} f_{lk}^{(j)}(x)\,dx \tag{15}$$

where $f_{lk}^{(j)}(x)$ is basis function number l of the longitudinal surface current for mode j, line k, and $c_{lk}^{(j)}$ is its corresponding basis function coefficient. The integral is defined over the cross section of the strip, S_k. The definition of modal characteristic impedance used in this work is [6]

$$Z_{kj}=\frac{\int \boldsymbol{E}_t^{(j)}\times\boldsymbol{H}_k^{(j)*}\cdot d\boldsymbol{S}}{|i_{kj}|^2} \tag{16}$$

where $\boldsymbol{E}_t^{(j)}$ is the total electric field for mode j and $\boldsymbol{H}_k^{(j)}$ is the partial magnetic field associated with the current on line k for mode j. The integral exists over the cross section of the shielded microstrip, which can be made large to approximate an open structure for the guided modes. It

should be noted that the definition of Z_{kj} is not unique due to the hybrid nature of the microstrip modes. Other impedance definitions are available [7], [8], any of which can be used in the circuit model. The eigenvoltages can be defined by using the modal characteristic impedances and eigencurrents, and along with the eigencurrents and propagation constants define the equivalent circuit.

IV. Examples

All eigencurrents, modal characteristic impedances, and effective dielectric constants used in this section were calculated using the full-wave technique outlined. At low frequencies, where these parameters are constant, the solution corresponds to the frequency-independent TEM solution. Thus if one can calculate the hybrid-mode parameters of microstrip using a full-wave solution, then the TEM parameters can easily be calculated by operating at low frequencies. Additionally, all examples were implemented using SPICE.

To verify the validity of the model, an example from the literature is analyzed. The example corresponds to a case studied by Chang [2] both experimentally and theoretically. The geometry is shown in Fig. 1. The line widths are 1.524 mm and are separated by 0.254 mm over a 0.254 mm substrate of epoxy glass ($\epsilon_r = 4.65$). For conciseness the presentation of effective dielectric constants, characteristic impedances, and eigencurrents is not given, but each parameter is nearly frequency independent to frequencies well over 10 GHz, owing to the low dielectric constant. The port termination notation is shown in Fig. 3, and port voltage calculations for the geometry in [2] are shown in Fig. 4. The results presented by Chang are difficult to accurately take from his figures, but good agreement is obvious upon comparison. It should be noted that the input voltage used here is an idealization of that used by Chang and this may account for any small discrepancies. The results were found using constant values of characteristic impedances, eigencurrents, and effective dielectric constants since they are relatively constant for this case to frequencies in excess of 10 GHz, and for the 1-ns-rise-time step (0 to 100 percent) only frequency components approximately $\leq$ 1GHz are required. This therefore corresponded to a TEM analysis.

All subsequent examples will be for the geometry of Fig. 5, selected as a case when modal dispersion occurs at relatively low frequencies such that the validity of the TEM approximation can be examined. The effective dielectric constants and characteristic impedances are plotted in Fig. 6 from 1 to 100 GHz. In comparison with [5], where little dispersion was indicated, it is seen that the lines become more dispersive when they are relatively wide (127 μm) and are situated over a high-permittivity substrate (Si, $\epsilon_r = 12$). In this case, dispersion becomes a factor at frequencies less than 20 GHz and the characteristic impedances (especially Z_{12}) show significant frequency dependence. Since the case examined in [5] was nearly dispersionless up to 100 GHz, it is expected that the TEM approximation would be valid for frequencies less than 100

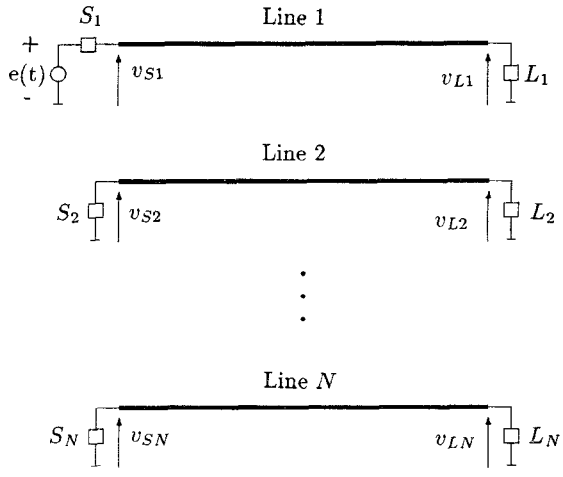

Fig. 3. Generalization of multiconductor microstrip. Line 1 is driven with emf $e(t)$. The termination at the source end of line k is referred to as S_k and that at the load as L_k.

GHz (as was shown). It is important to evaluate the accuracy of the TEM approximation for cases when dispersion becomes a factor.

Before comparing the results of a TEM analysis against a quasi-TEM analysis, one must first verify that a quasi-TEM approach is valid by examining the magnitudes of the longitudinal fields. Obviously if the longitudinal fields cannot be ignored, both the TEM and quasi-TEM approaches are invalid. For dispersive geometries such as the one considered, a full-wave analysis becomes more critical to verify that a quasi-TEM analysis is valid. Fig. 7 shows the magnitude squared of the longitudinal electric field integrated over the shield cross section (made large to approximate guided waves in an open structure) relative to the same quantities for the transverse electric fields. As a comparison, results are shown for the dispersionless case of [5] as well as for the dispersive case of two 127-μm-wide strips on Si described above. For the dispersionless case, the magnitude squared of the longitudinal electric field integrated over the cross section is less than 10^{-4} of the same quantities for the transverse field. For the dispersive structure, it is seen that the same ratios are much larger, and at 100 GHz the integral of the longitudinal field is nearly 20 percent of the integrals of the transverse fields for some field components. This is an indication that the quasi-TEM approximation is becoming poor and one might be required to use an alternative technique if signals with frequency components over 100 GHz are considered. Additionally, at frequencies over 100 GHz modes in the shielded structure that were evanescent at lower frequencies become propagating modes. The excitation of these higher order modes at discontinuities (terminations) is ignored in a quasi-TEM solution.

It is therefore seen that one must exercise caution when using the quasi-TEM approximation for picosecond pulses on microstrip over high-permittivity substrates. It is for these cases that using the full-wave approach will be most useful. In this example the quasi-TEM approximation (neglecting longitudinal fields) appears to be accurate up to

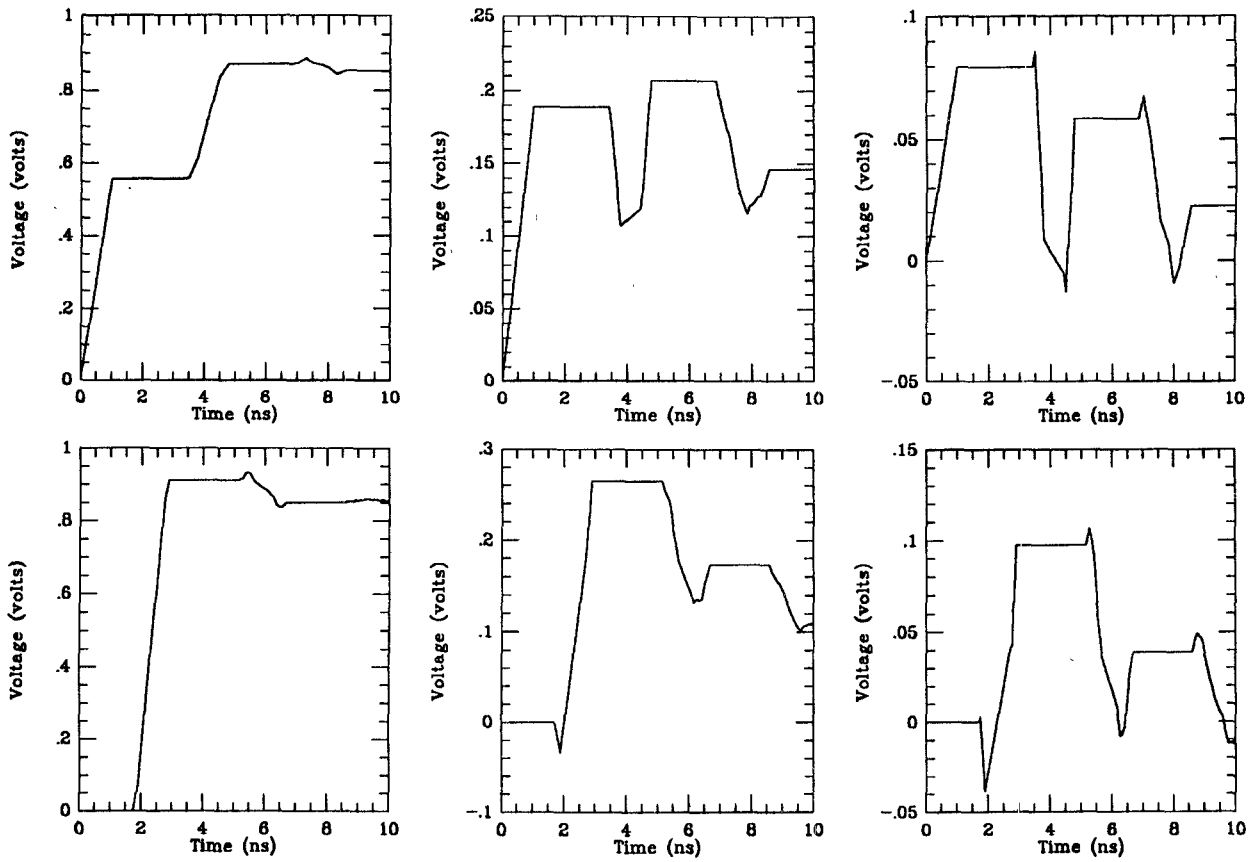

Fig. 4. Voltages at terminations of three-line geometry of Fig. 1. The input voltage $e(t)$ is idealized as a 1-ns-rise-time step as compared to that used in [2]. The top figures are for voltages at the ports of the driven end and the bottom figures are for voltages at the load end. From left to right the signals are on lines 1, 2, and 3, respectively. The line length is 30.48 cm (12 in). The terminations are resistors with $L_1 = L_3 = 310\ \Omega$, $L_2 = 367\ \Omega$, $S_1 = 50\ \Omega$, $S_2 = S_3 = \infty$ (open).

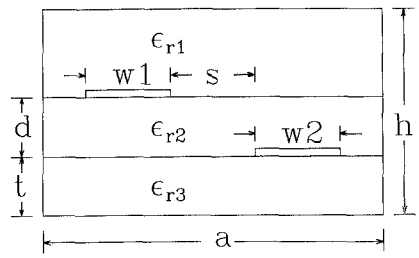

Fig. 5. Two-conductor microstrip geometry. The top line is referred to as line 1 and the bottom is line 2. Geometrical parameters: $w1 = w2 = t = d = 127\ \mu$m, $s = 381\ \mu$m, $a = h = 2.54$ cm, $\epsilon_{r2} = \epsilon_{r3} = 12$, and $\epsilon_{r1} = 1$.

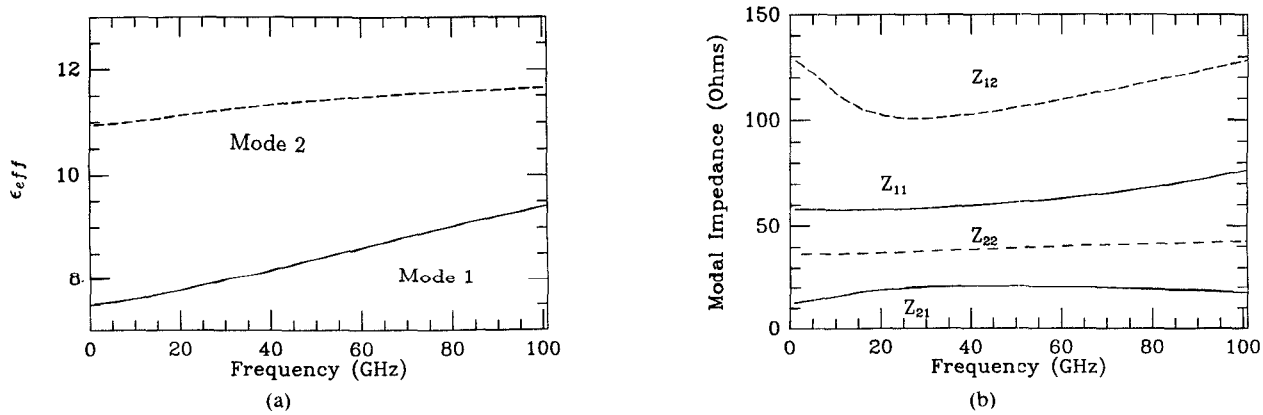

Fig. 6. The (a) effective dielectric constants and (b) characteristic impedances for Fig. 5. The characteristic impedance is denoted Z_{ij} for line i, mode j.

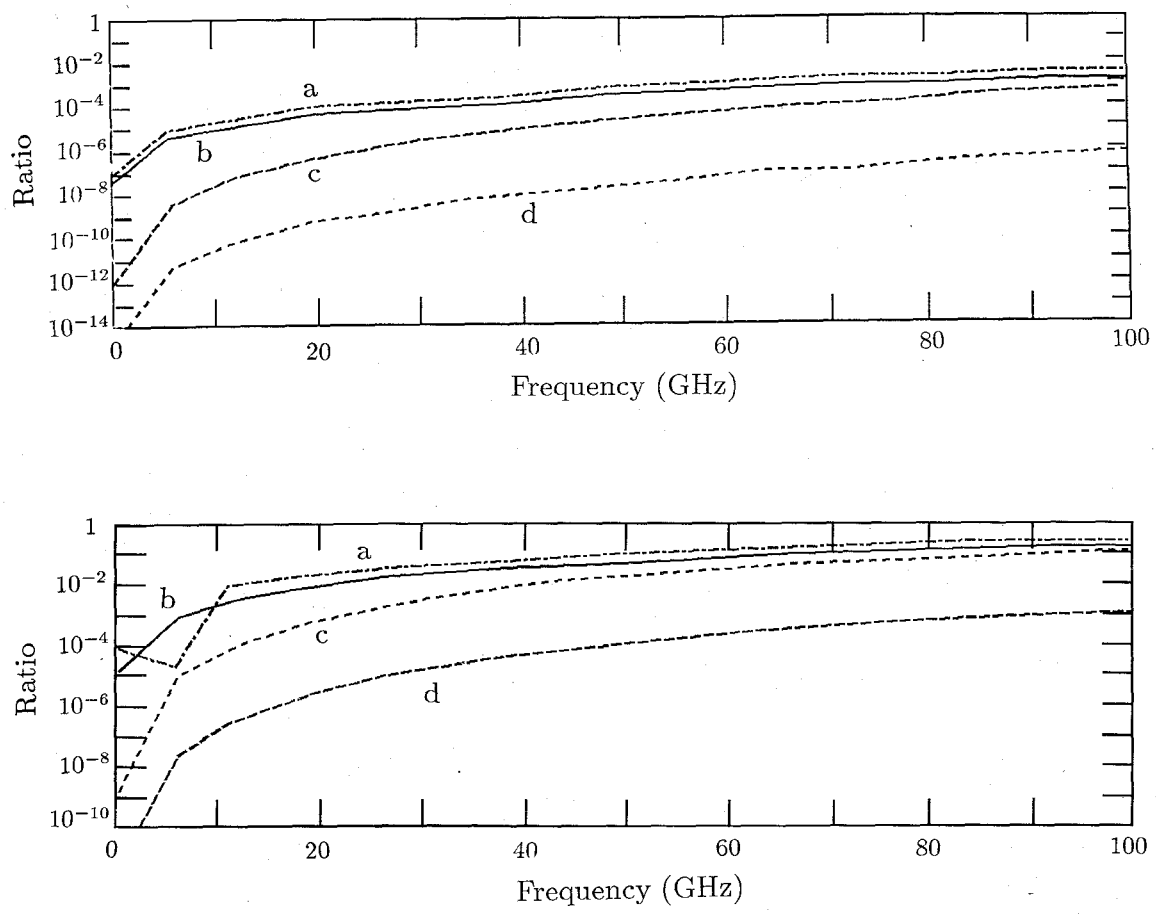

Fig. 7. The integral of the magnitude squared of the longitudinal electric field (E_z) divided by the integral of the magnitude squared of the transverse electric fields (E_x or E_y) with integrals over the shield cross section. The top figure is for the two line geometry in [5] ($w1 = w2 = t = d = 10$ μm, $\epsilon_{r2} = \epsilon_{r3} = 4$, $\epsilon_{r1} = 1$) and the bottom figure is for the parameters given in Fig. 5. The curves are as follows. *a*, mode 2 and E_x; *b*, mode 2 and E_y; *c*, mode 1 and E_x; *d*, mode 1 and E_y.

around 100 GHz although dispersion is significant at frequencies over 20 GHz, thus the need to distinguish between a TEM and a quasi-TEM mode representation. The presence of dispersion is not necessarily an indicator of the need to consider the longitudinal fields. To the contrary, these fields can often still be neglected and the frequency-dependent propagation accurately modeled by using a quasi-TEM as opposed to a TEM analysis.

Consider the geometry in Fig. 5 loaded with 50 Ω terminations at all ports, line 1 driven by a 1 V sinusoidal source, and 5 mm line lengths. The magnitude and phase of the voltage at the output ports of the two lines are shown in Fig. 8 for frequencies up to 100 GHz using the data in Fig. 6. The solid line corresponds to the TEM solution (using parameters from Fig. 6 at 1 GHz) and the dashed line uses frequency-dependent model parameters (quasi-TEM). It is seen for the case considered here that the TEM solution breaks down at frequencies close to 20 GHz and a frequency-dependent quasi-TEM analysis is required.

Time-domain results are now considered for pulses propagating on the lines in Fig. 5. Two different techniques can be used to perform such an analysis, depending on the geometry and signal speed. If the lines are long enough and the signal speeds fast enough, dispersion may become an issue. Using the equivalent circuit model, dispersive pulse propagation can be investigated for situations in which the lines are terminated in linear loads. The problem is solved at discrete frequencies, as was done in the calculation of Fig. 8, and then the frequency-domain data are converted to the time domain via the FFT. This technique is only applicable to cases for which linear loads are used. If the line lengths and signal speeds are such that dispersion is negligible, the model can be used to study pulse propagation on nonlinearly terminated lines. For such cases the model is implemented entirely in the time domain. Since the model is implemented in the time domain, the model parameters (eigencurrents, eigenvoltages, and mode speeds) are assumed to be frequency independent and the calculation reduces to a TEM signal propagation analysis. Obviously, this time-domain approach can also be used for linearly terminated lines when dispersion is negligible, as was done in the calculation of Fig. 4. To emphasize these points, two examples of pulse propagation on multiconductor transmission lines are studied. A dispersive case with linearly terminated lines is first investigated, followed by a nondispersive situation in which nonlinear terminations are used.

Consider the geometry in Fig. 5 with 10 mm line lengths. Assume all ports have 50 Ω terminations and line 1 is

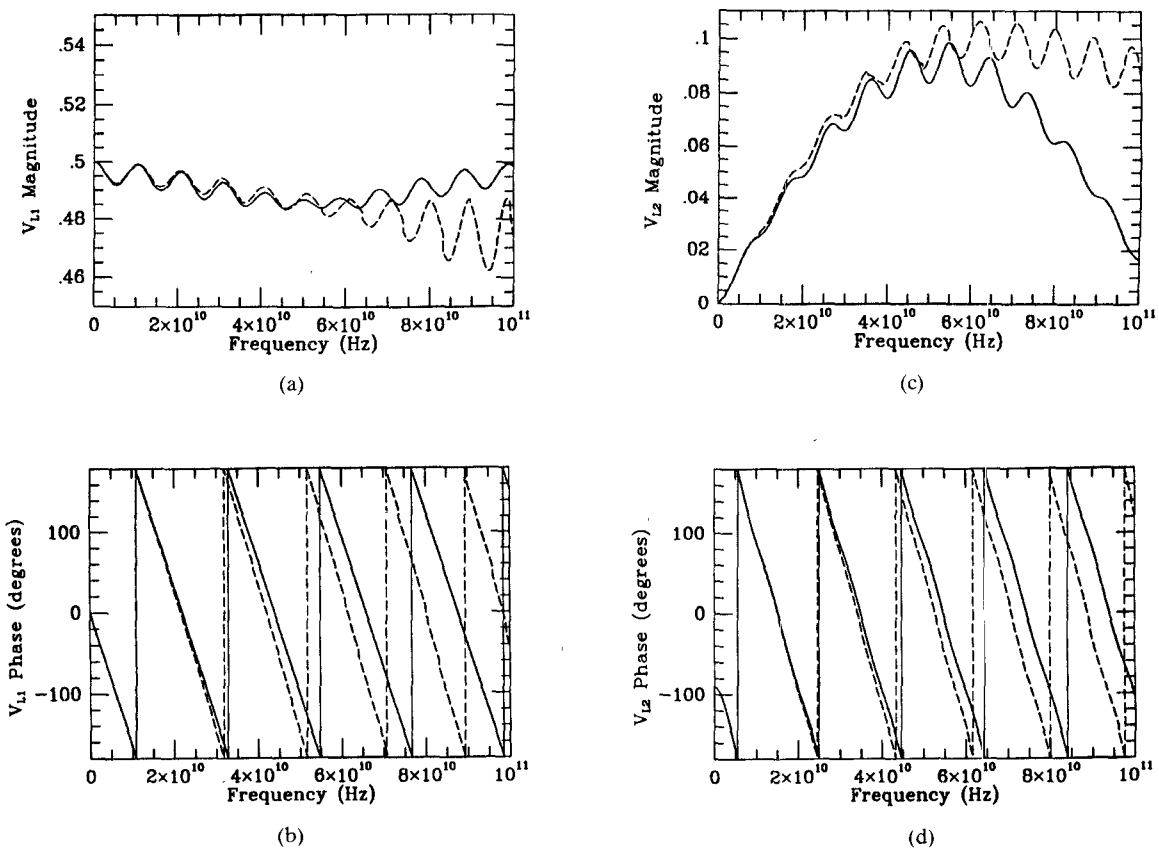

Fig. 8. Magnitude and phase of the voltage at the output ports of the two lines in Fig. 5. There are 50 Ω terminations at all ports and line 1 is driven by a 1 V sinusoidal signal at frequencies from 0 to 100 GHz. The lines are 5 mm long. The solid line corresponds to the frequency-independent TEM solution, and the dashed to the frequency-dependent quasi-TEM solution. (a), (b) Output of line 1. (c), (d) Output of line 2.

driven by a pulse with a 1 V peak amplitude, 15 ps rise and fall times (0–100 percent) and a 100 ps pulse width. Since the loads are linear, the dispersive problem can be analyzed by first working in the frequency domain. The computation is efficiently performed using the equivalent circuit model. The advantage of using this model coupled with a CAD package such as SPICE is that realistic, complicated linear terminations can easily be considered. For this calculation a 2048 point FFT was used with a sample spacing of 4.88 ps, producing a foldover frequency of 102.4 GHz. All 2048 points are used to model the pulse propagation along the line. The negative frequency components of the port voltages are the complex conjugate of the corresponding positive frequency components; thus only positive frequency components need be calculated using SPICE. SPICE was run at 33 discrete frequencies (from 0 to 102.4 GHz in 3.2 GHz increments) and the port voltages are approximated as being piecewise linear for frequencies between the computed points. The pulse voltage at the end of each line is plotted in Fig. 9. The solid line is the TEM result (constant mode speeds, eigenvoltages, and eigencurrents over the entire frequency range, 0 to 102.4 GHz, using values calculated at 1 GHz from a full-wave solution) and the dashed line considers dispersion. For the case considered here, the TEM solution approximates the dispersive quasi-TEM solution fairly well. For longer lines or faster signals the discrepancy should increase.

The circuit model for the multiconductor lines is now used to study pulse propagation on the microstrip model of Fig. 5 terminated in nonlinear loads. Since the loads are nonlinear, dispersion must be ignored when using the SPICE transmission line model. All model parameters used are those calculated at 1 GHz and a TEM analysis of the signal propagation is realized. Unlike the calculation above, the entire computation is performed in the time domain. Diodes are used as the device terminations and are assumed to obey the nonlinear $I-V$ relationship

$$i = 10^{-14}[\exp(40v) - 1]. \tag{17}$$

An input pulse with 0.5 ns rise and fall times and 1 ns width is used to study pulse propagation on the nonlinearly loaded lines and thus its frequency spectrum extends to approximately 2 GHz. Upon examining the dispersion curve and characteristic impedance for the geometry, one can see that the required parameters for the model are nearly frequency independent over the needed frequencies. Although not shown, the eigencurrents are also approximately constant. The pulse response for the coupled lines loaded with diodes, shown in Fig. 10, is similar to that in [3] for an analogous problem (two transmission lines with diodes as loads).

The CPU time and memory required by the model depend on the CAD package with which it is implemented. Each case shown above was calculated on a VAX 11/785

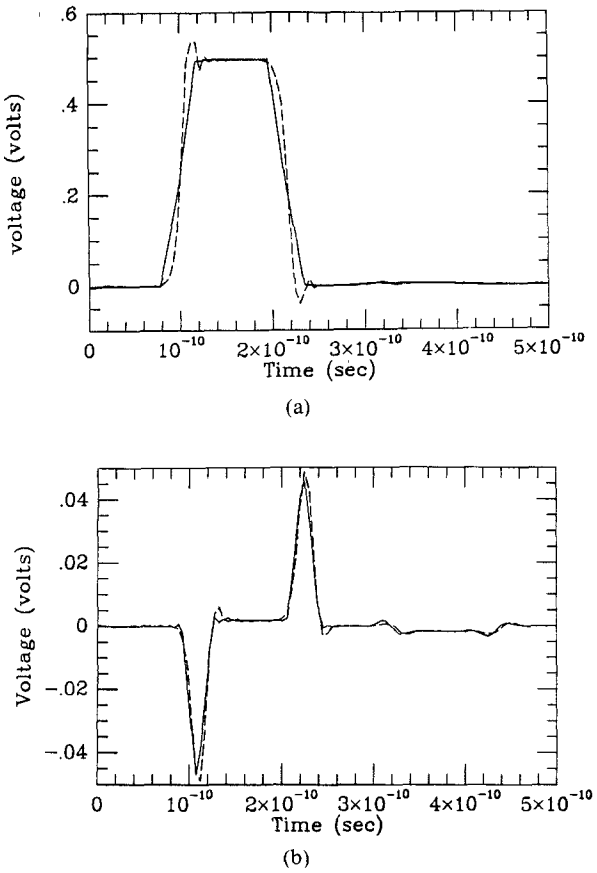

Fig. 9. Pulse response at the output ports of the two lines in Fig. 5. There are 50 Ω terminations at all ports and line 1 is driven by a 1 V pulse with 15 ps rise and fall times and a 100 ps width. The lines are 10 mm long. The solid line corresponds to the dispersionless TEM solution, and the dashed to the frequency-dependent quasi-TEM solution. (a) Output of line 1. (b) Output of line 2.

using SPICE, and none required more than 1 minute of CPU time (including the time for the FFT). This does not include the CPU time required to compute the frequency-dependent microstrip parameters. The speed of the spectral-domain technique is dependent on the complexity of the geometry and the number of basis functions and spectral terms used in the calculation. The SPICE program required about 2 Mbyte of RAM. To run the program, one has only to input the eigencurrents, effective dielectric constants, and modal characteristic impedances.

V. Conclusions

An equivalent circuit model for hybrid-mode multiconductor transmission lines has been presented. The equivalent circuit model parameters can be calculated through a TEM or a full-wave analysis. The full-wave approach allows one to use a dispersive quasi-TEM analysis once such an approximation has been validated. The model was used to simulate signal propagation on coupled microstrip with applications in high-speed integrated circuits. The form of the equivalent circuit model does not change with varying line length or frequency of operation. Within the

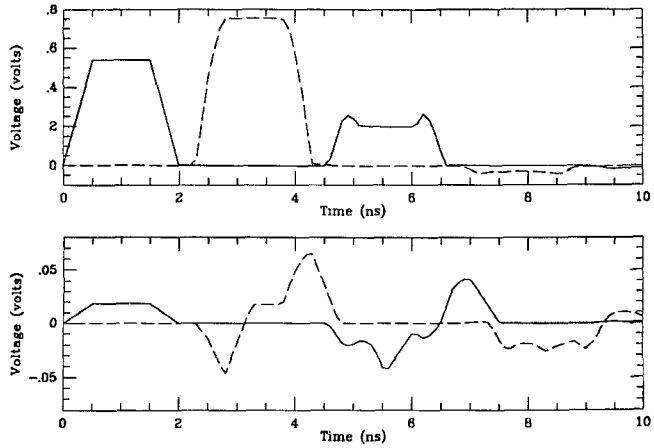

Fig. 10. Voltages at ports of geometry in Fig. 5 with 0.5 ns rise and fall times and 2-ns-wide 1 V amplitude pulse source, $e(t)$. The top figure is for voltages on line 1 and the bottom for line 2. The solid line represents voltages at the source end, and the dashed voltages at the load end. The loads, L_1 and L_2, are both diodes in series with 10 Ω resistors. The source terminations, S_1 and S_2, are both 50 Ω resistors. The lines are 30.48 cm long.

constraints of SPICE, dispersive linearly loaded lines and nondispersive nonlinearly loaded lines were analyzed. Loss was assumed negligible but could be included by using a more general CAD package. Since the model can easily handle a TEM as well as a quasi-TEM analysis of microstrip, it provides a means of evaluating the accuracy of the TEM approximation which neglects dispersion. The accuracy of the TEM approximation was investigated for time-harmonic as well as pulse signal propagation. For some cases examined, the time-harmonic signal propagation data obtained using the TEM approximation became quite inaccurate at frequencies in access of 20 GHz. The TEM approximation was adequate, however, for pulse propagation with 15 ps rise and fall time pulses on the geometries investigated. As the line widths, substrate dielectric constant, line lengths, and signal speeds increase, one would expect the effects of ignoring dispersion to become more pronounced.

References

[1] C. Wei, R. F. Harrington, J. R. Mautz, an T. K. Sarkar, "Multiconductor transmission lines in multilayered dielectric media," *IEEE Trans. Microwave Theory Tech.*, vol. MTT-32, pp. 439–449, Apr. 1984.

[2] F. Y. Chang, "Transient analysis of lossless coupled transmission lines in a nonhomogeneous dielectric medium," *IEEE Trans. Microwave Theory Tech.*, vol. MTT-18, pp. 616–626, Sept. 1970.

[3] A. R. Djordjevic, T. K. Sarkar, and R. F. Harrington, "Analysis of lossy transmission lines with arbitrary nonlinear terminal networks," *IEEE Trans. Microwave Theory Tech.*, vol. MTT-34, pp. 660–666, June 1986.

[4] T. Itoh, "Spectral domain immitance approach for dispersion characteristics of generalized printed transmission lines," *IEEE Trans. Microwave Theory Tech.*, vol. MTT-28, pp. 733–736, July 1980.

[5] Y. Fukuoka, Q. Zhang, D. P. Neikirk, and T. Itoh, "Analysis of multilayer interconnection lines for a high-speed digital integrated circuit," *IEEE Trans. Microwave Theory Tech.*, vol. MTT-33, pp. 527–532, June 1985.

[6] R. H. Jansen, "Unified user-oriented computation of shielded, covered and open planar microwave and millimeter-wave transmis-

sion-line characteristics," *Microwaves, Opt. and Acous.*, vol. 3, pp. 14–22, Jan. 1979.
[7] L. Weimer and R. H. Jansen, "Reciprocity related definition of strip characteristic impedance for multiconductor hybrid-mode transmission lines," *Microwaves and Opt. Tech. Lett.*, vol. 1, pp. 22–25, Mar. 1988.
[8] L. Carin and K. J. Webb, "Characteristic impedance of multilevel, multiconductor hybrid mode microstrip," *IEEE Trans. Magn.*, vol. 25, pp. 2947–2949, July 1989.
[9] J. R. Brews, "Transmission line models for lossy waveguide interconnections in VLSI," *IEEE Trans. Electron Devices*, vol. ED-33, pp. 1356–1365, Sept. 1986.
[10] V. K. Tripathi and J. B. Rettig, "A SPICE model for multiple coupled microstrips and other transmission lines," *IEEE Trans. Microwave Theory Tech.*, vol. MTT-33, pp. 1513–1518, Dec. 1985.
[11] O. A. Palusinski and A. Lee, "Analysis of transients in nonuniform and uniform multiconductor transmission line," *IEEE Trans. Microwave Theory Tech.*, vol. 37, pp. 127–138, Jan. 1989.
[12] A. R. Djordjevic, T. K. Sarkar, and R. F. Harrington, "Time-domain response of multiconductor transmission lines," *Proc. IEEE*, vol. 75, pp. 743–764, June 1987.
[13] V. K. Tripathi and A. Hill, "Equivalent circuit modeling of losses and dispersion in single and coupled lines for microwave and millimeter-wave integrated circuits," *IEEE Trans. Microwave Theory Tech.*, vol. 36, pp. 256–262, Feb. 1988.
[14] Touchstone Version 1.4, EEsof, 31194 La Boya Dr., Westlake Village, CA 91362.
[15] K. D. Marx, "Propagation modes, equivalent circuits, and characteristic terminations for multiconductor transmission lines with inhomogeneous dielectrics," *IEEE Trans. Microwave Theory Tech.*, vol. MTT-21, pp. 450–457, July 1973.

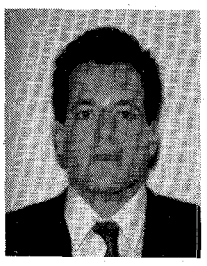

Lawrence Carin was born in Washington, DC., on March 25, 1963. He received the B.S., M.S., and Ph.D. degrees, all in electrical engineering, from the University of Maryland, College Park, in 1985, 1986, and 1989, respectively.

He is now an Assistant Professor with the Electrical Engineering Department at the Polytechnic Institute of New York. His present research interests include the analysis of electromagnetic waves in planar and quasi-planar structures used in high-speed integrated circuits.

Dr. Carin is a member of Tau Beta Pi and Eta Kappa Nu.

✠

Kevin J. Webb (S'80–M'84) was born in Stawell, Victoria, Australia, on July 7, 1956. He received the B.Eng. and M.Eng. degrees in communication and electronic engineering from the Royal Melbourne Institute of Technology, Australia, in 1978 and 1983, respectively, the M.S.E.E. degree from the University of California, Santa Barbara, in 1981, and the Ph.D. degree in electrical engineering from the University of Illinois, Urbana, in 1984.

Since 1984, he has been an Assistant Professor in the Electrical Engineering Department at the University of Maryland, College Park. His research interests include microwave and millimeter-wave integrated circuits, VLSI circuits, optoelectronics, numerical electromagnetics, and frequency selective surfaces.

Dr. Webb is a member of Tau Beta Pi, Eta Kappa Nu, and Phi Kappa Phi.